

## TiOPc Molecular Dislocation Networks as Nanotemplates for C<sub>60</sub> Cluster Arrays

Yinying Wei,<sup>†</sup> Steven W. Robey,<sup>‡</sup> and Janice E. Reutt-Robey<sup>\*†</sup>

Department of Chemistry and Biochemistry, University of Maryland, College Park, Maryland 20742, and National Institute of Standards and Technology, Gaithersburg, Maryland 20899-8372

Received April 23, 2009; E-mail: rrobey@umd.edu

Surface templated assembly is a key step for “bottom-up” construction of molecular based devices in molecular electronics, biosensors, and lately organic photovoltaic cells. Effective surface nanotemplates offer patterned adsorption or binding sites that accommodate additional functional components. Intensive efforts have been devoted to the fabrication of surface nanotemplates for operational devices and to investigations of molecular assembly processes involving these nanotemplates.<sup>1</sup> Elegant examples include 2D supramolecular porous networks, stabilized by directional noncovalent intermolecular interactions, such as C<sub>60</sub> molecules on a 2D porphyrin-based porous network and C<sub>60</sub> molecules steered by metal–organic coordination porous networks.<sup>2</sup> One limitation of surface templates produced by self-assembly is the relatively short (<several nanometer) pattern size imposed by molecular dimensions. Templates with a *ca.* 10 nm pattern repeat remain a challenge for both “bottom-up” construction and “top-down” lithography.<sup>3</sup>

Strategies for the efficient preparation of nanotemplates with 10 nm repeats need to be identified. Dislocations are important structural elements in crystalline materials that may be successfully harnessed for this length scale. Ultrathin metal films, for example, can form highly ordered arrays of dislocations to relieve the strain caused by the different lattice spacing between the metal films and the support.<sup>4</sup> Such misfit dislocation networks have already served as structural templates for metal nanoclusters and organic SAMs.<sup>5</sup> In principle, these dislocation networks are not limited to metal films but should be found also in thin molecular films with a suitable lattice mismatch to the substrate.

Here, we show that molecular films of titanyl phthalocyanine (TiOPc) can be processed to generate highly ordered misfit dislocation arrays with 15 nm repeats. These dislocation arrays are then used as a nanotemplate for the fabrication of C<sub>60</sub> cluster arrays. TiOPc is a technologically important molecular semiconductor due to its high hole mobility and optical band gap. Anisotropic TiOPc–TiOPc interactions contribute to a tendency to polymorphism in the bulk solid. In thin film form, however, this anisotropy helps to stabilize highly ordered dislocation networks. We then demonstrate the use of this dislocation network for the controlled assembly of C<sub>60</sub> cluster arrays. The dimensions of the resulting structure approach the nanophase segregated size targets for C<sub>60</sub>–TiOPc mixtures in photovoltaic applications.<sup>6</sup>

All molecular films were prepared *in situ* by physical vapor deposition and imaged at room temperature under ultrahigh vacuum conditions. Previously we have shown that controlled deposition flux allows for phase selection in TiOPc films on a Ag (111) substrate.<sup>7</sup> With the highest flux, TiOPc molecules (Figure 1a) form a quasi-periodic misfit dislocation triangular network on the surface,

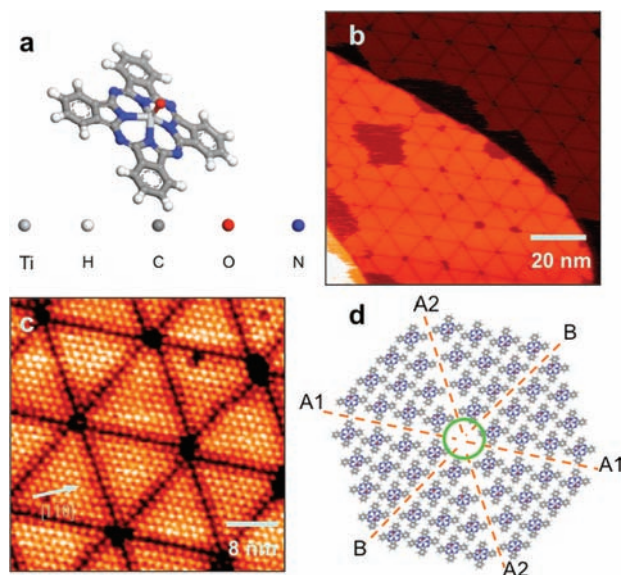


**Figure 1.** (a) Tilted view of the free TiOPc molecule. (b) STM image of TiOPc monolayer prepared by 0.4 ML/min. Flux reveals a regular network of triangular TiOPc domains. (c) Molecularly resolved STM image of the triangular network. Each molecule is represented by a bright spot in the image. (d) Structural model for the triangular network. For clarity, the domain network is truncated to show only 4 molecules (out of the 11–13) along the domain boundaries.

as shown in Figure 1b. As per the magnified image of Figure 1c, these triangular domains display a remarkable uniformity in size with 11–13 molecules packing along each side creating a domain length of *ca.* 15 nm. According to the model proposed in Figure 1d, all molecules within one triangular domain have the same orientation with an estimated 30°-tilting angle from the Ag surface. Molecules in the adjacent domains are oriented oppositely, thus creating highly stabilizing domain boundaries (A1, A2, and B in Figure 1d). At room temperature, the triangular network structure is stable, transforming to the hexagonal TiOPc phase only upon thermal annealing at 390 K.

We now test this dislocation structure as a nanotemplate for C<sub>60</sub> assembly. First we note that C<sub>60</sub> molecules can select from three types of surface sites: above the TiOPc triangular domains, along the domain boundaries (dashed lines in Figure 1d), and at the intersection of six adjacent triangular domains (circle in Figure 1d). Only at the latter intersection will the C<sub>60</sub> molecules interact directly with the Ag (111) surface. At this domain intersection, the area of exposed silver surface is determined by the packing of TiOPc molecules. Ideally terminated domains (Figure 1d) leave a Ag region of 3 to 4 nm<sup>2</sup> that is sufficient to directly accommodate 3 close-packed C<sub>60</sub> molecules. Many domains are not ideally terminated, missing 3–6 TiOPc molecules at the domain intersection. Such

<sup>†</sup> University of Maryland.

<sup>‡</sup> National Institute of Standards and Technology.

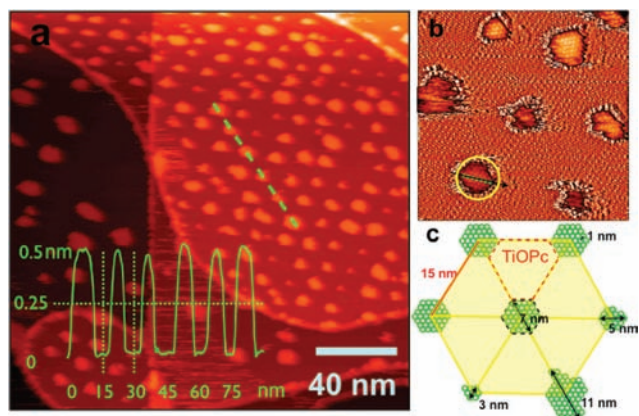


**Figure 2.** (a) Large scale STM image of  $C_{60}$  cluster array on TiOPc triangular dislocation networks. Inset is the line profile of the six  $C_{60}$  clusters along the dashed line. (b) STM image of  $C_{60}$  clusters shown as a differential image to enhance molecular resolution. (c) Size distribution of the diameter for  $C_{60}$  clusters;  $N$  represents the number of  $C_{60}$  molecules along the diameter. (d) Schematic illustration of the nanophase segregated  $C_{60}$  and TiOPc domains.

domain intersections (see Figure 1b and 1c) expose bare Ag (111) regions with  $8\text{--}12\text{ nm}^2$  in area.

Deposition of 0.2 ML  $C_{60}$  onto triangular TiOPc networks immediately results in the formation of ordered arrays of  $C_{60}$  nanoclusters (Figure 2a). The spacing between  $C_{60}$  clusters is  $14.0 \pm 1.0\text{ nm}$ , corresponding to the characteristic dimension of each triangular TiOPc domain. Each  $C_{60}$  cluster is positioned at the intersection of six TiOPc domains. The topographic line profile of  $C_{60}$  and TiOPc structures (Figure 2a dashed line) confirms that  $C_{60}$  molecules directly contact the Ag surface. Under room temperature imaging conditions,  $C_{60}$  clusters show dynamic structure variations on the 30 s time scale of STM image acquisition. As shown in Figure 2b, clusters contain a “core” of close-packed  $C_{60}$  molecules. The “rim” of the  $C_{60}$  cluster appears noisy in the STM images, indicating more weakly attached  $C_{60}$ . There are some variations in the size and shape of the clusters, with hexagonal clusters generally appearing more stable and easily imaged and elliptical clusters appearing somewhat less stable. This is consistent with  $C_{60}$ 's well-known hexagonal close packing, which energetically favors hexagonal shaped clusters.

The  $C_{60}$  clusters thus occupy a quasi-periodical superlattice with a spread in cluster size. We quantify the size of an individual cluster by its diameter at the point of maximum width, as illustrated in Figure 2b. A histogram of the  $C_{60}$  cluster width distribution, given in the Supporting Information, reveals a  $7 \pm 2\text{ nm}$  average cluster size and a 7 nm most probable size. Diameters of the  $C_{60}$  clusters span the 1–12 nm range and are accommodated by the TiOPc network structure, as depicted in Figure 2c. Effectively, both the  $C_{60}$  nanocluster and the TiOPc triangular domain must fit within the 15 nm repeat of the misfit dislocation network. The average 7 nm  $C_{60}$  cluster diameter leaves TiOPc domains of similar size. Consequently,  $C_{60}$  deposition on the TiOPc film template results in a pattern of nanophase-separated  $C_{60}$  and TiOPc domains with a characteristic domain size of 7 nm. We note that this 7 nm dimension is comparable to the exciton diffusion length in a molecular semiconductor. Achieving nanophase segregation of molecular semiconductors on this length scale is believed to be a crucial step toward improving the efficiency of small-molecule photovoltaic cells.

The resulting nanophase-separated TiOPc- $C_{60}$  film structures are quite robust. Once  $C_{60}$  cluster arrays are formed on the TiOPc dislocation network, the binary film can be heated to 420 K without degrading the structure. In fact, this binary film structure is considerably more stable than the original TiOPc template, for which the dislocation network is removed by thermal annealing at temperatures of just 390 K.

In conclusion, we have shown that a dislocation network in a molecular film provides a convenient template for generating pattern features on the several-nanometer length scale, bridging the practical limits of “bottom up” and “top down” strategies. We have used TiOPc, a molecular semiconductor with anisotropic interactions, to generate a molecular film with a characteristic pattern repeat size of 15 nm. This structure then served as the nanotemplate for a superlattice of  $C_{60}$  clusters with characteristic diameters of 7 nm. As a result,  $C_{60}$  deposition on the TiOPc film template forms a pattern of nanophase-separated  $C_{60}$  and TiOPc domains with a characteristic domain size of 7 nm. Once the length scale of the phase separation is established by this method, it should propagate to some film thickness before decaying. Studies to examine how well the templated phase separation can be maintained to multilayer films are currently being planned. Misfit dislocations in thin molecular films are a common phenomena<sup>8</sup> that can be more generally exploited for nanopatterning on the 10 nm length scale.

**Acknowledgment.** This work has been supported by the National Science Foundation under Surface Analytical Chemistry Grant CHE0750203 and the Department of Commerce through the NIST small grants program.

**Supporting Information Available:** Figure of size distribution of the diameter for  $C_{60}$  clusters. This material is available free of charge via the Internet at <http://pubs.acs.org>.

## References

- (a) Sanchez, L.; Otero, R.; Maria Gallego, J.; Miranda, R.; Martin, N. *Chem. Rev.* **2009**, *109* (5), 2081. (b) Stohr, M.; Wahl, M.; Spillmann, H.; Gade, L. H.; Jung, T. A. *Small* **2007**, *3* (8), 1336. (c) Surin, M.; Samori, P. *Small* **2007**, *3* (2), 190. (d) Otero, R.; Eciija, D.; Fernandez, G.; Gallego, J. M.; Sanchez, L.; Martin, N.; Miranda, R. *Nano Lett.* **2007**, *7* (9), 2602. (e) Yoshimoto, S.; Tsutsumi, E.; Narita, R.; Murata, Y.; Murata, M.; Fujiwara, K.; Komatsu, K.; Ito, O.; Itaya, K. *J. Am. Soc. Chem.* **2007**, *129*, 4366. (f) Ait-Mansour, K.; Buchsbaum, A.; Ruffieux, P.; Schmid, M.; Groning, P.; Varga, P.; Fasel, R.; Groning, O. *Nano Lett.* **2008**, *8*, 2035. (g) Yoshimoto, S.; Honda, Y.; Ito, O.; Itaya, K. *J. Am. Soc. Chem.* **2008**, *130*, 1085. (h) Kong, X. H.; Yang, Y. L.; Lei, S. B.; Wang, C. *Surf. Sci.* **2008**, *602* (3), 684.
- (a) Spillmann, H.; Kiebele, A.; Stohr, M.; Jung, T. A.; Bonifazi, D.; Cheng, F. Y.; Diederich, F. *Adv. Mater.* **2006**, *18*, 275. (b) Stepanow, S.; Lingenfelder, M.; Dmitriev, A.; Spillmann, H.; Delvigne, E.; Lin, N.; Deng, X. B.; Cai, C. Z.; Barth, J. V.; Kern, K. *Nat. Mater.* **2004**, *3*, 229.
- (a) Okazaki, S. *Int. J. High Speed Electron. Syst.* **2006**, *16* (1), 375. (b) Huie, J. C. *Smart Mater. Struct.* **2003**, *12* (2), 264.
- (a) Hamilton, J. C.; Foiles, S. M. *Phys. Rev. Lett.* **1995**, *75*, 882. (b) Barth, J. V.; Brune, H.; Ertl, G.; Behm, R. J. *Phys. Rev. B* **1990**, *42*, 9307. (c) Ling, W. L.; Hamilton, J. C.; Thurmer, K.; Thayer, G. E.; de la Figuera, J.; Hwang, R. Q.; Carter, C. B.; Bartelt, N. C.; McCarty, K. F. *Surf. Sci.* **2006**, *600*, 1735. (d) Diaconescu, B.; Nenchev, G.; Jones, J.; Pohl, K. *Microsc. Res. Techn.* **2007**, *70*, 547.
- (a) Fruchart, O.; Klaua, M.; Barthel, J.; Kirschner, J. *Phys. Rev. Lett.* **1999**, *83*, 2769. (b) de la Figuera, J.; Pohl, K.; Schmid, A. K.; Bartelt, N. C.; Hrbek, J.; Hwang, R. Q. *Surf. Sci.* **1999**, *435*, 93. (c) Strocio, J. A.; Pierce, D. T.; Dragoset, R. A.; First, P. N. *J. Vac. Sci. Technol.* **1992**, *10*, 1981.
- Tsuzuki, T.; Shirota, Y.; Rostalski, J.; Meissner, D. *Sol. Energy Mater. Sol. Cells* **2000**, *61*, 1.
- Wei, Y. Y.; Robey, S. W.; Reutt-Robey, J. E. *J. Phys. Chem. C* **2008**, *112* (47), 18537.
- (a) Budevskii, E.; Staikov, G.; Lorenz, W. *J. Electrochemical phase formation and growth*; VCH: Weinheim; New York, 1996. (b) Cyganik, P.; Buck, M.; Wilton-Ely, J.; Woll, C. *J. Phys. Chem. B* **2005**, *109* (21), 10902.

JA903055W